Geophys. J. Int. (2005) **161,** 268–282 doi: 10.1111/j.1365-246X.2005.02582.x

A re-evaluation of the great Aleutian and Chilean earthquakes of 1906 August 17

Emile A. Okal

Department of Geological Sciences, Northwestern University, Evanston, IL 60201, USA. E-mail: emile@earth.nwu.edu

Accepted 2004 October 27. Received 2004 October 17; in original form 2004 February 28

SUMMARY

We investigate two great earthquakes that occurred in the Aleutian Islands and Chile, within 30 min of each other, on 1906 August 17, based on a collection of seismograms compiled shortly after the events by scientists at Strasbourg. The method of Preliminary Determination of Focal Mechanisms (PDFM) is applied to 14 mantle waves from seven stations, in order to resolve the moment tensors of the two shocks. It is complemented by examination of body wave polarities at Japanese stations to lift the remaining indeterminacy in focal mechanism. The Chilean earthquake, occurring second, is a regular subduction event, whose moment (2.8×10^{28} dyn cm) is revised downwards from previous estimates (except Kanamori's), suggesting that its rupture did not involve more than ~200 km of fault. The Aleutian earthquake, occurring first, has a larger moment (3.8×10^{28} dyn cm), but features mantle wave radiation patterns and body wave polarities incompatible with both underthrusting at the Aleutian subduction zone and tensional buckling at the outer rise. Rather, we suggest that it is an intraplate, somewhat deeper (~50 km) earthquake: this is supported by tentative relocation of available arrival times north of it. The origin of the earthquake may be related to the presence of the Bowers ridge north of the Amchitka pass in the epicentral area. Finally, hydrodynamic simulations using our source mechanisms support the observation that the Chilean event was the source of the reported transpacific tsunami; the report of a 3.5-m wave at Maui constitutes a misassociation, as its timing is shown to be non-causal for both events.

Key words: focal mechanisms, historical earthquakes, tsunamis.

1 INTRODUCTION AND GENERAL BACKGROUND

On 1906 August 17, two earthquakes later assigned magnitudes in excess of 8 by Gutenberg & Richter (1954) took place within 30 min of each other, in the Aleutian Islands and Chile, respectively. Their coincidence in time, which we take as fortuitous, remains unique in the annals of historical seismology for events of this magnitude, and has led to significant confusion regarding the relative size of the two shocks and even their respective role in generating a Pacific-wide tsunami.

The exceptional character of the simultaneous occurrence of a duo of such large earthquakes was not lost on the leaders of the International Seismological Association, who entrusted the Imperial Central Station for Earthquake Research in Strasbourg[1] with the compilation and publication of a worldwide collection of copies of the original records. The result was a remarkable set of records from 78 stations, published on heavy photographic paper and accompanied by meticulous descriptions of their instrument characteristics (Rudolph & Tams 1907). The present study uses this data set to conduct a modern seismological reassessment of these two events, including an inversion of their focal mechanism using the Reymond & Okal (2000) method of Preliminary Determination of Focal Mechanisms (PDFM). We conclude that the Aleutian earthquake was the larger of the two, but that it could not have been an interplate thrust earthquake. Rather, we propose that it is somehow associated with the lateral heterogeneity in the subduction process located at the Amchitka pass, in a pattern reminiscent of the 1994 Shikotan earthquake in the Kuril Islands. The far-field tsunami was generated by the Chilean event.

1.1 The earthquakes

Various reports summarized by Rudolph & Tams (1907) establish that the Aleutian earthquake occurred in the vicinity of Amchitka island around 00:11 GMT, whereas the Chilean shock took place near Valparaiso at 00:41 GMT. Epicentral parameters were estimated for the Aleutian shock by Zöppritz (1906) as 50°N, 180°E, 00:10:47 and by Omori (1907) as 50°N, 175°E, 00:11:44. Estimates for the Chilean event are derived from Steffen (1907a) who does not

[1] Then Straßburg im Elsaß, (Prussian) Imperial Lands. Throughout this paper, names and spelling of geographical sites will reflect present political boundaries.

quote a precise epicentre, but only an origin time as 00:41:22 GMT. The earthquakes are listed by Gutenberg & Richter (1954) at 51°N, 179°E, 00:10:42 and 33°S, 72°W; 00:40, respectively, based on Gutenberg's own calculations, documented on his personal notepads (Goodstein *et al.* 1980).

In very general terms, the 1906 Aleutian earthquake occurred at the eastern end of the rupture zone of the great 1965 Rat Island earthquake (Stauder 1968a; Beck & Christensen 1991), essentially a location close to the recent event on 2003 November 17. The 1906 Chilean earthquake is generally interpreted as located in the same area as the 1822 and 1985 Valparaiso events (Lomnitz 1970; Comte *et al.* 1986).

There are no usable reports of the local effects of the Aleutian earthquake, because of the remoteness of its epicentral area (Rudolph & Tams 1907). By contrast, the Chilean event is well documented, notably by Steffen (1907a,b). Many investigators have interpreted his descriptions and maps in terms of a possible rupture length, but their estimates vary greatly, from 245 km (Kelleher 1972) to 330 km (Nishenko 1985) and even 365 km (Comte *et al.* 1986). The longer rupture would make the 1906 event significantly larger than the 1985 and probably the 1822 earthquakes.

1.1.1 The tsunami

While tsunami waves were detected throughout the Pacific in the aftermath of the two shocks, there remains some uncertainty as to their exact source. As compiled by Solov'ev & Go (1984), the tsunami was relatively minor along the Chilean coast, with run-up not exceeding 1.5 m. This figure is comparable to reports by Plafker (1985) following the 1985 event, although it may have to be corrected for transient coastal uplift, reported by Steffen (1907b) to be in the 80-cm range. The 1906 tsunami was detected on tidal gauges as far as Japan, with a maximum peak-to-peak amplitude of 44 cm. In the Hawaiian Islands, run-up was reported to have reached 1.5 m at Hilo and, most surprisingly, 3.5 m on Maui, while the tidal gauge amplitude in Honolulu did not exceed 10 cm. These reports led Lomnitz (1970) to propose that the transoceanic tsunami was generated by the Aleutian, rather than Chilean, shock. However, Solov'ev & Go (1984) argue that tsunami arrival times can be reconciled only with a Chilean origin. The matter is made more confused by inconsistencies in the timescales superimposed by Solov'ev & Go (1984) on the marigrams reproduced in their monograph. Also, as detailed in the Appendix, the inundation at Maui occurred too early to be associated with either earthquake.

In view of these uncertainties, we went back to the six original marigrams published by Honda *et al.* (1908). For each of them, we verified that the time is correctly expressed in local time (GMT +9 in Japan; GMT −10:30 in Hawaii; GMT −8 in California) by matching the oscillation of the tide, as computed from the interactive web site (`www.shom.fr`) of the *Service Hydrographique et Océanographique de la Marine* of the French Navy. This revealed a number of errors in the timescales of fig. 29 (p. 129) of Solov'ev & Go (1984): times are labelled correctly at the Japanese stations, but for San Francisco, San Diego and Honolulu the local time (labelled with the Russian letter *Tche*) and the universal (GMT) time (labelled *h*) are both off by 12 hr. The onsets of the oscillations on figures of Honda *et al.* (1908) are in agreement with travel times from the Chilean epicentre at all five sites. No signal is present on the California marigrams at the times expected for a hypothetical Aleutian tsunami. At the Japanese and Hawaiian stations, such arrivals would fall before the beginning of the time-series plotted; however, it can be reasonably assumed that, had such signals been detectable, Honda *et al.* (1908) would have adjusted the time windows to include them.

Thus, we uphold the interpretation of Solov'ev & Go (1984) and reject that of Lomnitz (1970): the Aleutian earthquake did not generate a detectable far-field tsunami. On the other hand, the Chilean event generated a tsunami recorded Pacific-wide, including in Japan with decimetric amplitudes. This is an important observation, as we will conclude that the Aleutian earthquake is the greater of the two in terms of seismic moment.

1.1.2 Magnitude and moment estimates

Gutenberg & Richter (1954) assigned magnitudes $M = 8.0$ and 8.4 to the Aleutian and Chilean shocks, respectively. Abe & Noguchi (1983a,b) revised these estimates downwards, in an attempt to make them more in line with present-day M_s values; Comte *et al.* (1986) further proposed $M_s = 8.3$ for the Chilean event. However, because of saturation of spectral amplitudes at 20 s (Geller 1976), M_s is not expected to be an accurate measure of earthquake size in this range of magnitudes.

Kanamori (1977) lists a moment estimate of 2.9×10^{28} dyn cm for the Chilean earthquake, based on 'the aftershock area'; he probably means isoseismal areas, because to our best knowledge, no detailed epicentral information is available for aftershocks. Abe (1981) and later Comte *et al.* (1986) proposed moment estimates of 4×10^{28} and 6.6×10^{28} dyn cm respectively, based on tsunami magnitudes, but these probably give too much weight to the unrelated run-up at Maui and as such are biased upwards. Scaling laws (Geller 1976) would associate Kanamori's (1977) estimate with a shorter rupture than given by Comte *et al.* (1986; 185 versus 365 km), who used the extent of coastal uplift reported by Steffen (1907a). However, the detailed examination of Steffen's (1907b) isoseismal map reveals a more concentrated zone of maximum intensity (IX), extending no more than 200 km and more in line with Kanamori's moment estimate.

More recently, Okal (1992a) derived mantle magnitudes M_m for the Aleutian earthquake from Wiechert records at Uppsala; he noted a large discrepancy between Rayleigh and Love spectral amplitudes, which could not be reconciled with a regular interplate thrust mechanism. He was unable to extract surface waves of the Chilean earthquake from the Uppsala (UPP) records, further noted the absence of any detectable second passages and suggested a possible value of 1.5×10^{28} dyn cm for the Aleutian earthquake, assuming its mechanism was that of an outer-rise shock.

2 RELOCATION

To our best knowledge, the only systematic effort at relocating the 1906 shocks is the work of Boyd & Lerner-Lam (1988) for the Aleutian event. These authors used Rudolph & Tams' (1907) data set to derive an epicentre at 51.05°N, 179.69°W, with an error estimate of 50 km along the arc. However, their technique specifically included an arc proximity constraint, expressing the tacit assumption of interplate thrust faulting, which, as mentioned above, may be inadequate (Okal 1992a).

Here, we use the iterative interactive relocation algorithm of Wysession *et al.* (1991), an approach admittedly less sophisticated than Boyd & Lerner-Lam's (1988), but making use of a Monte Carlo algorithm, which injects Gaussian noise (with standard deviation σ_G) into the data set. We interpret the first and second advance phases in table III ('1. u. 2. Vorläufer') of Rudolph & Tams (1907) as *P* and *S* times, respectively.

In the case of the Aleutian event, a set of 42 *P* and 44 *S* times converges on an epicentre at 50.60°N, 178.36°E with an

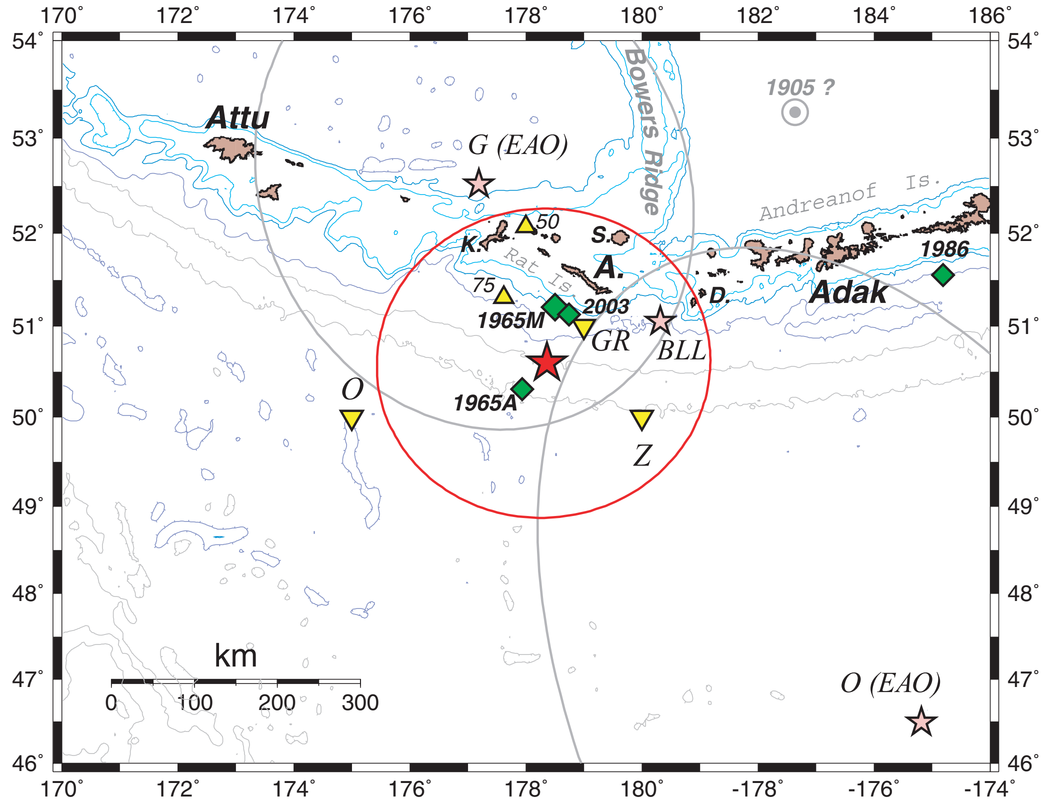

Figure 1. Location of the Aleutian event of 1906 August 17. The large star (with nearly circular Monte Carlo ellipse) is the result of our relocation, based on 86 times from Rudolph & Tams (1907). The upward-pointing triangles are epicentres obtained by imposing a 75- or 50-s maximum residual threshold. The downward-pointing triangles are epicentres proposed by Omori (1907) (*O*), Zöppritz (1906) (*Z*) and Gutenberg & Richter (1954) (*GR*). The smaller stars show other computerized relocations, by Boyd & Lerner-Lam (1988) (*BLL*) and our relocations (with Monte Carlo ellipses) of Omori's [*O*(*EAO*)] and Gutenberg's [*G*(*EAO*)] data sets. The diamonds are the epicentral relocations by Engdahl *et al.* (1998) of the large recent events of 1965 [main shock (M) and outer-rise aftershock (A)] and 1986, and the National Earthquake Information Center (NEIC) solution for the 2003 event. The bull's-eye symbol shows our relocation of the possibly deeper 1905 earthquake. The islands of Amchitka (*A.*), Kiska (*K.*), Semiposochnoi (*S.*) and the Delarof group (*D.*) are identified. Bathymetric contours are at 1000, 2000, 4000 and 6000 m.

origin time of 00:11:00 GMT. The rms residual, $\sigma = 34.9$ s, would be regarded as outrageous by the standards of today, but should be considered acceptable given the obvious scatter in the data. The solution is remarkably robust under the Monte Carlo algorithm, yielding an uncertainty ellipse with semi-axes approximately 200 km long, for $\sigma_G = 35$ s $= \sigma$ (Fig. 1). The data set has no depth resolution, with constrained-depth epicentres being essentially undistinguishable in the depth range 10–100 km. The ellipse includes Boyd & Lerner-Lam's (1988) epicentre and, remarkably, the early estimate by Zöppritz (1906), who used only four stations. Omori's (1907) epicentre lies only 35 km outside the ellipse.

Following Boyd & Lerner-Lam (1988), we further explored the effect of imposing a cap on acceptable residuals r: we find that relocated epicentres move north, as the maximum $|r|$ is decreased, to 51.31°N, 177.62°E for $|r| \leq 75$ s, and 52.07°N, 178.00°E for $|r| \leq 50$ s, both within the original Monte Carlo error ellipse. The latter provides a reasonable constraint on the epicentre: while it gives an adequate picture of the location of the event along the arc, it provides no resolution in the transverse direction; the earthquake could be an interplate thrust event, or an outer-rise earthquake similar to the nearby event of 1965 March 30 (Stauder 1968b; Beck & Christensen 1991), or a deeper shock displaced arcwards of the trench and reminiscent of the 1994 Kuriles earthquake (Kikuchi & Kanamori 1995).

We also inverted the more limited set of 29 times on which Omori (1907) based his epicentral estimate and the 36 times listed on Gutenberg's notepads (Goodstein *et al.* 1980). For the Omori data set and after discarding three stations, we find a more southerly epicentre, at 46.49°N, 175.19°W; however, it is poorly constrained and its Monte Carlo ellipse ($\sigma_G = 35$ s) grazes our own solution. Gutenberg's data set converges to a back-arc location (52.52°N, 177.19°E), with an rms residual of 17.8 s, only 75 km from the solution we achieve by imposing $|r| \leq 50$ s (Fig. 1). It is impossible to understand the origin of the 210-km discrepancy between Gutenberg's solution and our inversion of his data set, as we do not know how Gutenberg achieved his solution, i.e. which station(s) he may have discarded, or weighted low, in the process. However, it would be legitimate to assume that he was forcing the epicentre into the Aleutian seismic belt, in effect implementing a pencil-and-paper version of what Boyd & Lerner-Lam (1988) later called an 'arc-proximity constraint'.

In summary, Fig. 1 confirms that the 1906 Aleutian earthquake occurred near Amchitka island, at the eastern end (and epicentral area) of the 1965 rupture. Its location is not resolved in the direction transverse to the arc, but both the relocation of Gutenberg's data set and our own relocation excluding large residuals would suggest a trend towards a back-arc location.

Relocation efforts are less successful in the case of the Chilean earthquake, whose records fall in the coda of the Aleutian shock,

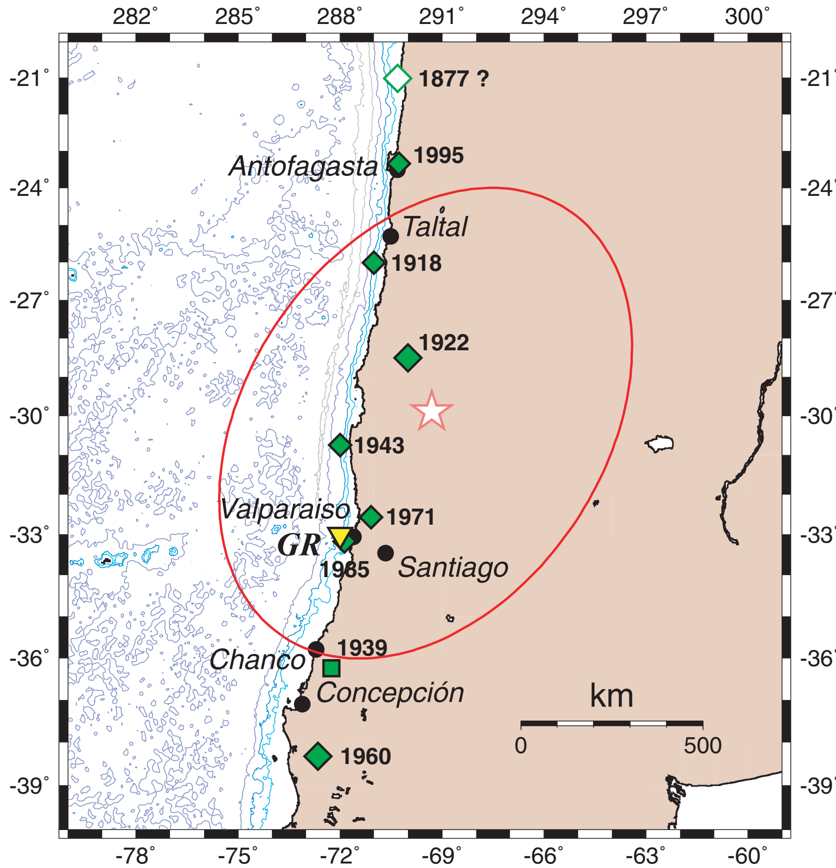

Figure 2. Same as Fig. 1 for the Chilean event of 1906 August 17. The open star is the result of our formal relocation; note the large Monte Carlo ellipse, which includes more than 1000 km of coastline. The inverted triangle (*GR*) is the epicentral location of Gutenberg & Richter (1954). Epicentres of other large shocks are from Engdahl *et al.* (1998) starting with the 1960 event and Gutenberg & Richter (1954) for older ones. The location of the pre-instrumental 1877 event is estimated and shown by an open diamond. The square identifies the 1939 Chillan intraplate event.

resulting in picks of a clearly much lower quality. Rudolph & Tams (1907) do not report any second advance phases (‘2. Vorläufer’), which suggests the possibility of confusion between *P* and *S* times; in addition, most European stations fall in the core shadow. As a result, our best location uses only six stations and converges on an inland location at 29.9°S, 69.3°W, OT 00:41:01 with an rms residual of 28.7 s. Most significantly, the Monte Carlo ellipse ($\sigma_G = 35$ s) has a NNE–SSW semi-axis of 670 km. The epicentre could be anywhere along the coast from Taltal in the north to Chanco in the south (Fig. 2). As in the case of the Aleutian event, we attempted to invert the data set of 11 *P* and two *S* times on Gutenberg's notepads (Goodstein *et al.* 1980), but the algorithm failed to converge.

In summary, we could not relocate the Chilean event from available data sets; we will use the approximate epicentre (33°S, 72°W) proposed by Gutenberg & Richter (1954), which falls inside the zone of maximum felt intensity (MM IX) (Steffen 1907b).

3 MOMENT TENSOR INVERSION

We apply to both shocks the method of PDFM introduced by Reymond & Okal (2000), following an idea originally expressed by Romanowicz & Suárez (1983). In simple terms, it consists of inverting only the amplitude part of the spectra of mantle waves (both Rayleigh and Love) at a limited number of stations, while discarding the phase information. As discussed by Okal & Reymond (2003), this method is particularly well adapted to the analysis of historical earthquakes, because the correct interpretation of phase spectra requires accurate relative timing between stations and adequate epicentral information, both of which may not be available. In addition, information on the polarity of recordings at historical stations is occasionally lost; in particular, in Rudolph & Tams' (1907) data set, it is given only for the Japanese stations (TOK and OSK).

As pointed out by Romanowicz & Suárez (1983), Reymond & Okal (2000) and Okal & Reymond (2003), the method has an inherent indeterminacy of $\pm 180°$ on both the strike and slip angles of the best-fitting double couple. It can be lifted by considering independent evidence such as polarization of body waves or interpretation in the geological context.

3.1 Choosing the stations

Because Reymond & Okal (2000) showed that the PDFM method can provide reliable solutions with as few as three stations offering adequate azimuthal coverage, we elected to choose a limited number of high-quality records from the data set of Rudolph & Tams (1907) and discarded many more, as a result of poor contrast, loss of the seismic trace going off scale after body waves, use of undamped (Milne type) instruments, exceedingly low gains, or rapid fall-off at long periods. Also, we emphasized high-quality records and adequate azimuthal coverage over redundancy at a given azimuth. In the end, we selected 14 phases from seven stations providing reasonable

Table 1. List of records used in the moment tensor inversion.

Station			Aleutian Event				Chilean Event			
Code	Name	Instrument	Distance Δ (°)	Azimuth ϕ_s (°)	Back azimuth β (°)	Phases used	Distance Δ (°)	Azimuth ϕ_s(°)	Back azimuth β (°)	Phases used
API	Apia, Samoa	Wiechert	65.2	170	354	G_1	90.5	253	124	R_1
GEO	Washington, DC, USA	Bosch	68.4	54	319	R_1	71.9	356	176	R_1, G_1
OSK	Osaka, Japan	Omori					157.1	281	93	R_1
STR	Strasbourg, France	Wiechert	80.3	354	6	R_1, G_1				
TIF	Tbilisi, Georgia	Zöllner	79.2	327	27	R_1, G_1	130.1	61	259	G_1
TOK	Tokyo, Japan	Omori	31.9	257	49	R_1				
UPP	Uppsala, Sweden	Wiechert	68.3	350	12	R_1, G_1				

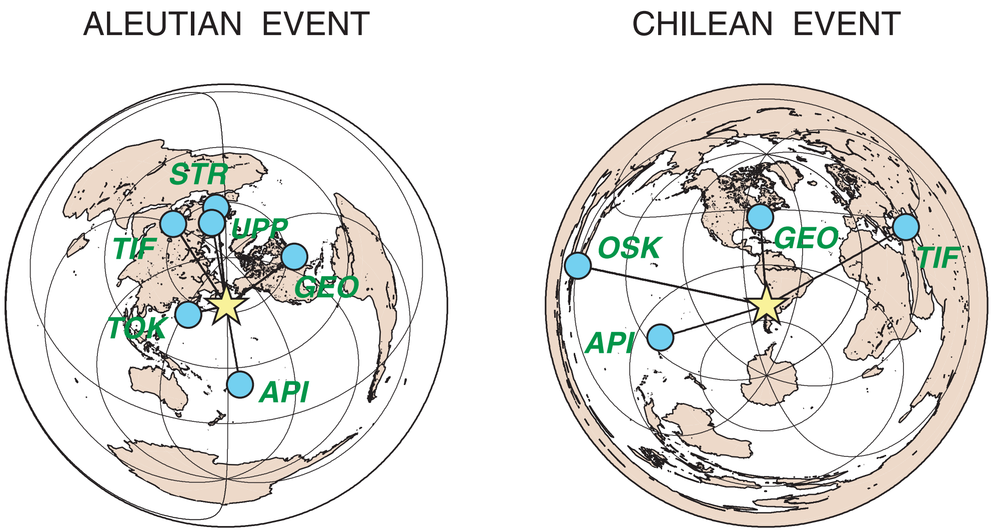

Figure 3. Stations used in the inversions of the Aleutian (left) and Chilean (right) events. Each map is an equidistant azimuthal projection of the whole Earth, centred on the epicentre of the event (shown as a star).

azimuthal coverage from both epicentres, as compiled in Table 1 and mapped on Fig. 3. Figs 4 and 5 show examples of the mantle phases used in the inversion. Records were digitized and interpolated at $\delta t = 1$ s. Instrumental characteristics were retrieved from Rudolph & Tams (1907).

Following the technique described by Reymond & Okal (2000), the records were processed through the M_m algorithm (Okal & Talandier 1989, 1990) and the resulting spectral amplitudes smoothed by a cubic spline in the 100–200 s period range. Inversions were carried out at five periods between 100 and 180 s under an interactive iterative process; a small amount of damping was used to stabilize the process.

3.1.1 *Results: Aleutian event*

For the Aleutian event, we use six stations sampling 110° in azimuth (Fig. 3). The result of the inversion is shown on Fig. 6; our solution provides a nearly perfect fit to all spectral amplitudes, with the exception of the lowest-frequency Love wave at STR. The four possible orientations of the best-fitting double couple (mechanisms I–IV) are shown on the right of Fig. 6. Fig. 7 explores the influence of depth (which remains constrained during the inversion) on the solution. The quality of fit, expressed by the rms residual, is essentially constant. As expected, the inversion becomes poorly conditioned (Tarantola 1987) for the shallowest sources, expressing the classical surface singularity of the excitation of any seismic mode or wave by the M_xz and M_yz components of the moment tensor, with the inverted mechanism turning into pure dip-slip and the amplitude of M_0 artificially increased. Note that the condition number also increases around 70 km. At that depth, the coefficient K_0 characterizing the excitation of Rayleigh waves by the component M_zz (Kanamori & Stewart 1976) vanishes for $T \approx 146$ s and remains small at the other periods. As M_zz does not excite Love modes, this results in a singularity that turns the best-fitting double couple into nearly pure normal faulting. Our preferred solution, featuring a reliable, well-conditioned inversion and a good rms value, is at 50 km, with $M_0 = 3.8 \times 10^{28}$ dyn cm. Note that it is essentially stable between 40 and 60 km.

In order to study the effect of any remaining uncertainty in instrument responses and following Okal & Reymond (2003), we tested the robustness of the solution when station gains are increased or decreased, one at a time, by 25 per cent. We find that the inverted moment varies between −13 and +12 per cent about its unperturbed value and that the geometry of the best-fitting double couple is rotated from the original solution at most 8° in the formalism of Kagan (1991). We also verified that our results do not depend on the amount of damping introduced in the inversion. We conclude that the solution is indeed robust.

Most importantly, our inversion confirms that the event cannot be an interplate thrust earthquake. Okal (1992a) had noticed that the large Love-to-Rayleigh spectral ratio at UPP was incompatible with such a geometry. We confirm this trend at station STR, which is only 10° in azimuth from UPP (see for example the remarkable Love wave record on Fig. 4). When imposing the geometry of the

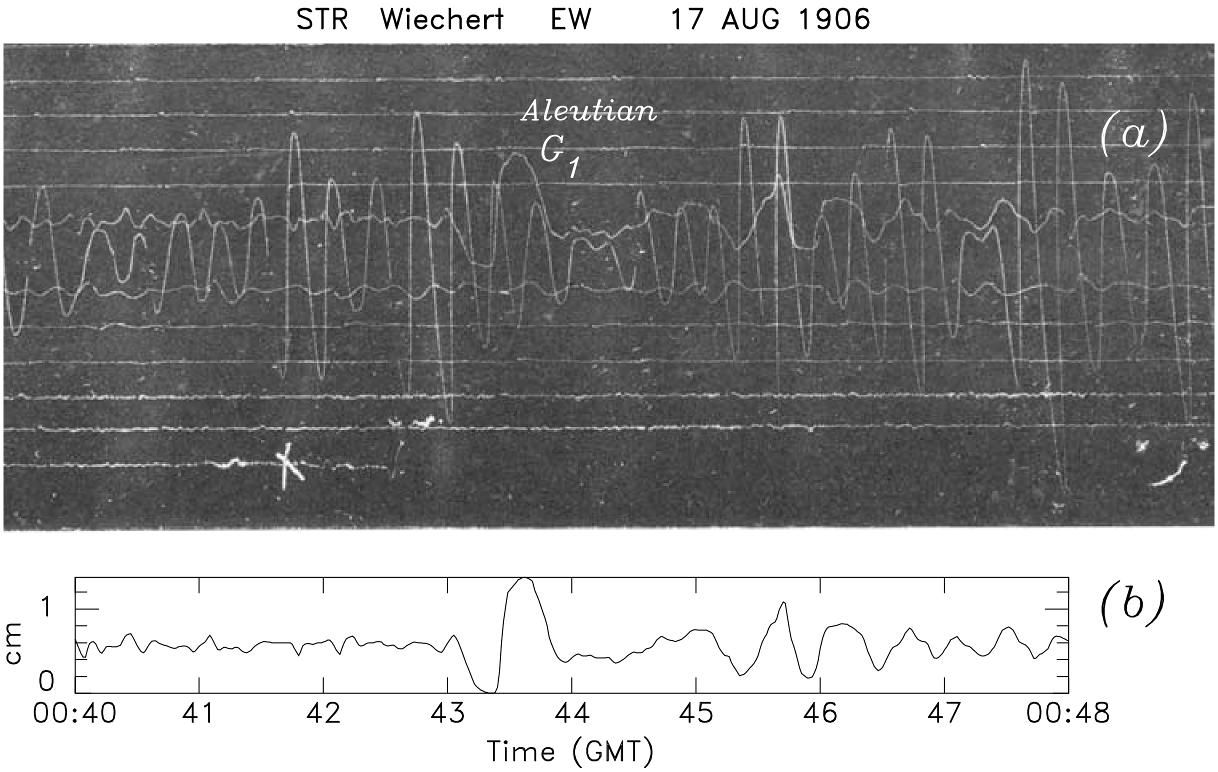

Figure 4. East–west Wiechert record of the Aleutian G_1 wave at Strasbourg. (a) Original record reproduced from Rudolph & Tams' (1907) collection. Note the exceptional sharpness of the phase. (b) The same after digitization, suppression of pen curvature and slant, and equalization to $\delta t = 1$ s.

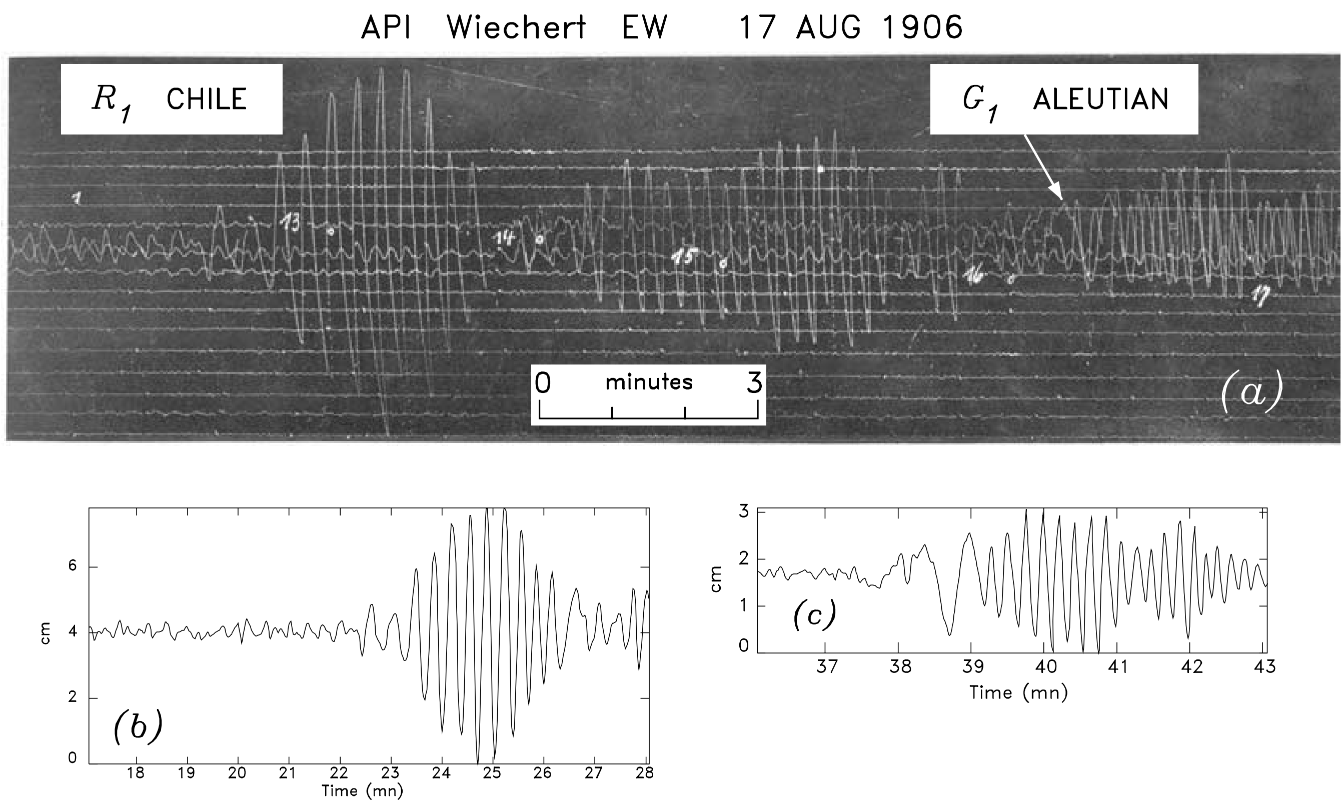

Figure 5. East–west Wiechert record at Apia. (a) Section of the original record showing prominently the Rayleigh arrival from the Chilean event (left). The Aleutian Love wave (G_1) is also discernable on the right, even though it is overprinted by the coda of the Chilean Rayleigh wave, about 1 hr later. The numbers (13 to 17) refer to hour marks expressed in local time (GMT −11 : 27 : 04). (b) and (c) Time-series used in the inversion after digitization, suppression of pen curvature and slant, and equalization to $\delta t = 1$ s.

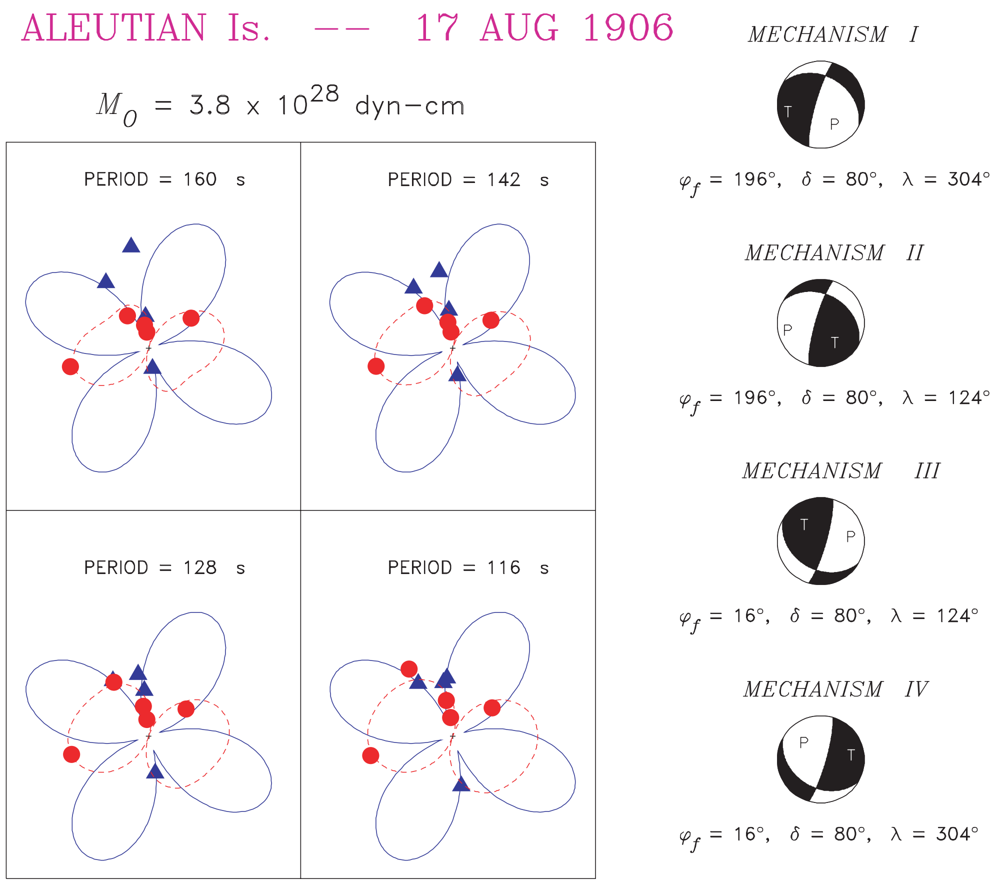

Figure 6. Result of the Preliminary Determination of Focal Mechanisms (PDFM) inversion for the Aleutian event. The four panels on the left give examples of the fit of spectral amplitudes at representative periods. On each diagram, the solid line is the theoretical azimuthal radiation pattern (north up) of Love waves by the inverted mechanisms. The solid triangles are the observed Love spectral amplitudes at individual stations. The dashed line and solid dots similarly represent the Rayleigh waves. The scales vary between periods but are common inside each panel to Love and Rayleigh waves, observed and predicted values. The beach-balls on the right show the four possible geometries of the best-fitting double couples resulting from the double indeterminacy in the preferred solution.

1965 Rat Island main shock ($\phi_f = 290°$, $\delta = 18°$, $\lambda = 139°$; Wu & Kanamori 1973; also close to that of the recent event on 2003 November 17) and optimizing the scalar moment, we find that the radiation pattern is very poorly fit, as it predicts large Rayleigh-to-Love ratios in Europe (UPP, STR) and nodal Rayleigh waves at TOK, all of which are contradicted by our observations; the rms residual more than doubles, to 32.3 in the units of Fig. 7. The mechanism of Stauder (1968b)[2] for a normal faulting outer-rise event ($\phi_f = 104°$, $\delta = 47°$, $\lambda = -118°$) fares only marginally better, poorly matching radiation patterns of both Rayleigh and Love waves.

3.1.2 Resolving the indeterminacy

The seismograms in Rudolph & Tams (1907) generally do not include information on the polarity of the recording and thus the direction of first motions cannot be assessed. Fortunately, the seismograms reproduced in Omori (1907) do carry this information, revealing decisive, impulsive first motions to south and west (away from the source) for the *P* waves at TOK and OSK (Fig. 8). For *S* waves, a sharp initial eastward motion is read at TOK and OSK, and a probable northward motion at TOK. In Table 2, we use the formalism of Kanamori & Stewart (1976) to compute the source radiation coefficients expected from mechanisms I–IV. To predict *S* polarities on the horizontal components, we further assume that the incidence angles at the stations are steep enough to allow a direct rotation of the *SV* and *SH* components (Okal 1992b).

Only mechanism I correctly predicts the polarities of the *P*-wave and eastward *S*-wave first motions. We therefore assign mechanism I ($\phi_f = 196°$, $\delta = 80°$, $\lambda = 304°$) to the Aleutian event. We also note that the interplate thrust mechanism (in the geometry of the 1965 or 2003 events) predicts a strong westward impulse for *S* and that the outer-rise mechanism would predict a dilatational *P* wave.

3.1.3 Results: Chilean event

For the Chilean event, we use four stations sampling 95° in azimuth (Fig. 3). The result of the inversion is shown on Fig. 9. As in the case of the Aleutian event, the rms residual is insensitive to depth in the 20–60 km range (Fig. 10), with the solution best conditioned between 30 and 50 km. By analogy with the 1985 Valparaiso earthquake, we favour a 40-km centroid depth, representative of interplate events in the area. The inverted moment ($M_0 = 2.8 \times 10^{28}$ dyn cm) is in excellent agreement with the figure of 2.9×10^{28} dyn cm proposed by Kanamori (1977) on the basis of isoseismal

[2]Caution should be given to the fact that Stauder (1968a,b) plots focal mechanisms with a convention exactly opposite the one adopted universally, i.e. he shades the quadrants with 'dilatational', 'rarefied', or 'kataseismic' first arrivals.

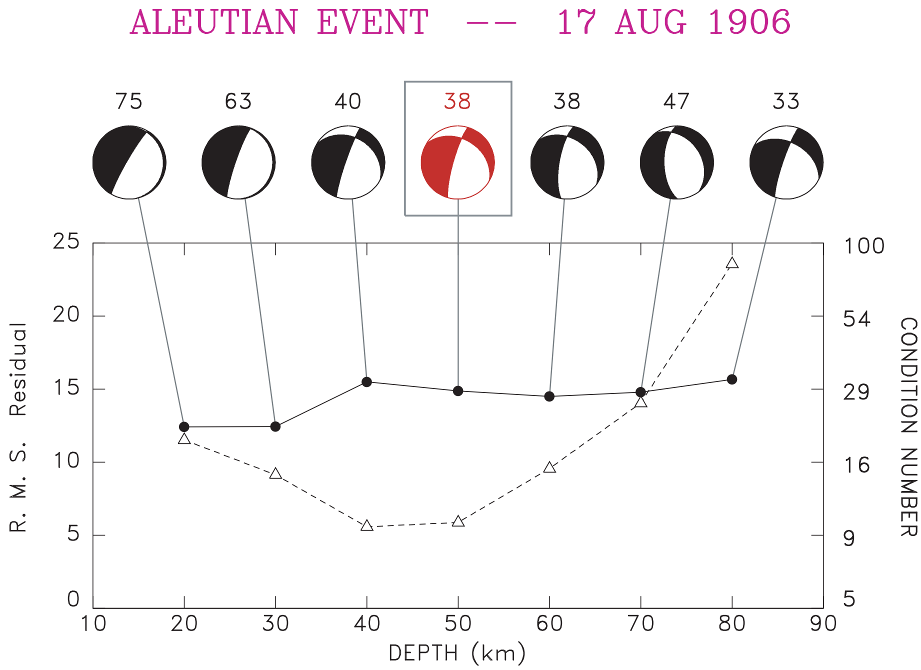

Figure 7. Influence of depth on the results of the inversion for the Aleutian event. At each of the seven constrained depths, the focal mechanism (closest to mechanism I) of the best-fitting double-couple is shown with the inverted moment in units of 10^{27} dyn cm above the beach-ball. The dots (connected by the solid line) show the rms residual of the inversion (in arbitrary units common to all depths; left scale). The triangles (connected by the dashed line) show the condition number of the inversion (logarithmic scale on the right). The preferred solution at 50 km depth is emphasized.

reports. We again verified the stability of our results with respect to the amount of damping introduced in the inversion and also explored the effect of uncertainties in instrument responses. Because of the smaller number of stations, the solution can vary by ±20 per cent in moment and rotate as much as 25°, under the assumption of an error of 25 per cent in the gain at API, the station with greatest importance, as defined by Minster *et al.* (1974). However, the solution does retain its shallow thrust geometry, most of the variation being in the strike and slip angles.

Our solution departs slightly (18° in Euler space in the formalism of Kagan 1991) from that of the nearby 1985 Valparaiso earthquake and we find this difference resolvable, as the 1985 geometry increases the rms residual under the best-fitting scalar moment by a factor of more than 2.

3.1.4 Resolving the indeterminacy

In the case of the Chilean earthquake, no first motion polarities are available, as its body waves fall within the coda of the surface waves of the Aleutian event. From a tectonic standpoint, the earthquake could be interpreted as an interplate thrust event by selecting mechanism I on Fig. 9 ($\phi_f = 3°$, $\delta = 15°$, $\lambda = 117°$), or as an intraplate normal faulting event similar to the 1939 Chillan earthquake in the central valley, by selecting mechanism IV. The latter is within the range of geometries given by Beck *et al.* (1998) for the 1939 event. We favour the former interpretation on account of the damage reports (Steffen 1907b), which feature isoseismals centred on the coast line rather than the central valley, as well as coastal uplift between 32°S and 35°S.

4 DISCUSSION

Our inversions by the PDFM method establish that the Aleutian earthquake was the greater of the two large events of 1906 August 17. However, it was not an interplate thrust earthquake, but rather an intraplate one, probably at some depth, and thus the transpacific tsunami was generated by the Chilean earthquake. We discuss separately our results for each event, in the framework of their tectonic province.

4.1 The Chilean event: regular subduction of an ∼200-km fragment of the Nazca Plate

Our results regarding the Chilean event are relatively straightforward, the earthquake representing an episode of simple subduction of the Nazca Plate under the central Chile coast. With respect to the 1985 event, we derive a slightly less pure mechanism, with a shallower dip and a slight component of strike-slip. These discrepancies could be genuine, or they could be an artefact of the source complexity suggested by felt reports (Steffen 1907b). Our principal result concerns the inverted seismic moment, $M_0 = 2.8 \times 10^{28}$ dyn cm, equivalent to that proposed by Kanamori (1977), but significantly less than proposed by Abe (1981) and Comte *et al.* (1986), and difficult to reconcile with the interpretation of the latter of a homogeneous rupture along a 365-km fault.

As discussed above, we believe that Steffen's (1907b) isoseismal data could support a shorter rupture (≈200 km), extending from 32.3°S to 34.1°S. We can only offer speculation as to the relationship of this segment to previous historical earthquakes (e.g. 1751, 1880), as the interpretation of their ruptures varies significantly among different researchers (Lomnitz 1970; Kelleher 1972; Comte *et al.* 1986).

4.2 The Aleutian event: a 1994-Kuriles-type earthquake?

Our most interesting results relate to the Aleutian event. We confirm our original suggestion (Okal 1992a) that it cannot be a regular

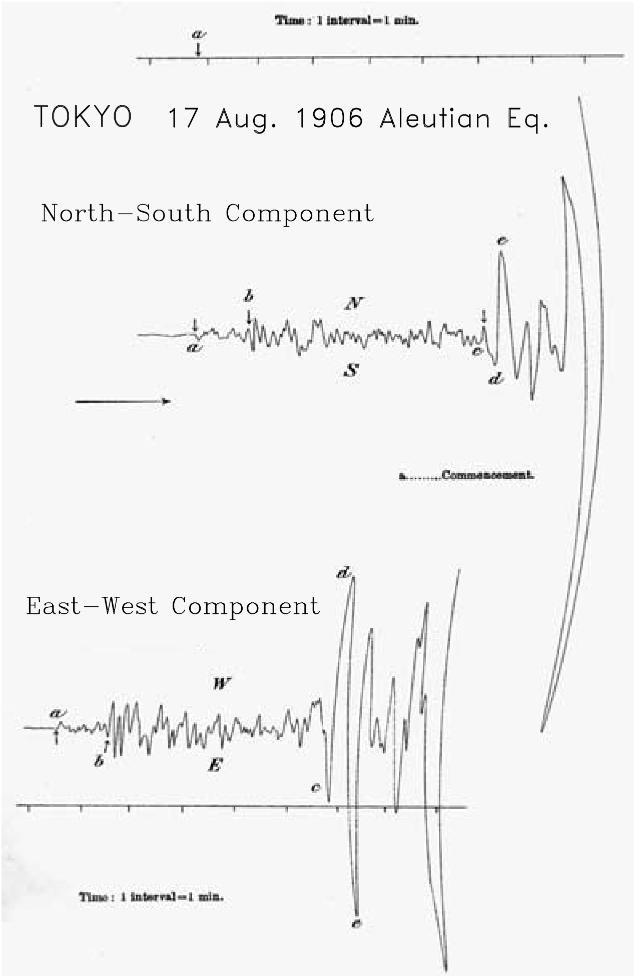

Figure 8. Close-up of the Omori records at TOK (after Omori 1907). Note the definitive first motion of P to the south and west (a). Regarding the first motion of S, the time marks, although irregular, allow the correlation of motion on the two components. We thus verified that the small peak at the last arrow on the NS component matches the time of the large trough marked c on the WE record. Thus, the large, sharp higher-frequency motion to the east is accompanied by a smaller motion to the north.

interplate subduction earthquake, whose geometry would be incompatible not only with the surface wave radiation patterns, but also with the sharp eastward initial deflection of the S waves at OSK and TOK (Fig. 8). In addition, the polarity of P waves at the same stations rules out the tensional mechanism of an outer-rise event, which we had suggested as a possible explanation of the Love-to-Rayleigh ratio at Uppsala (Okal 1992a).

Neither of the two possible geometries of mechanism I is readily interpretable in the direct vicinity of the trench and we propose that the 1906 Aleutian event took place further north, below or beyond the arc, in a context reminiscent of the 1994 Kuriles earthquake under Shikotan island (Kikuchi & Kanamori 1995; Tanioka *et al.* 1995). That shock tore the Pacific Plate under the arc at a very similar depth and had a moment only slightly less than derived here for the 1906 Aleutian earthquake (3.0×10^{28} dyn cm).

As documented by the Harvard catalogue, seismic moment release around the proposed 1906 hypocentre is presently very low, but this should not necessarily preclude the occasional occurrence of a very large event; we note for example the relative spaciotemporal isolation of the great 1938 Banda Sea intraplate earthquake at a similar centroid depth (Okal & Reymond 2003).

The interpretation of the 1906 event as displaced towards the backarc and the Bering sea is supported by the definite northward trend of our relocations when placing a cap on acceptable residuals and by our own relocation of Gutenberg's data set. We also note that Gutenberg & Richter's (1954) catalogue does include four neighbouring large shocks ($M \geq 6.9$) listed either at 60 km depth, or below and north of the arc, on 1905 February 14, 1912 January 4, 1913 March 31 and 1929 July 7. We relocated these events based on arrival times listed in Gutenberg's notepads (Goodstein *et al.* 1980) for the first three and the International Seismological Survey (ISS) for the last one. Only the 1905 event (given $M = 7\frac{3}{4}$ by Gutenberg & Richter 1954) converges north of the arc, to 53.27°N, 177.36°W (Fig. 1). As the data set cannot resolve depth and modern-day seismicity at that location is exclusively intermediate-depth, it is legitimate to consider that the 1905 earthquake could be at least 100 and possibly 200 km deep. The relocation is good ($\sigma = 5.77$ s on 14 stations) but many arrivals, primarily of S waves, had to be discarded. On the other hand, the Monte Carlo ellipse (drawn with the same $\sigma_G = 35$ s used throughout this study for turn-of-the-century events) does extend to the interplate seismic belt and the 1905 earthquake could be an interplate thrust event, as concluded by Boyd & Lerner-Lam (1988), although they were once again working under their self-imposed arc-proximity constraint. The other three shocks relocate to the line of shallow subduction and there is nothing in their traveltime data sets to suggest that they are anything but interplate thrust events. In short, there is some possible, but weak, evidence in the historical record for intraplate activity at large magnitudes arcwards of the central Aleutians.

The 1906 earthquake took place in a general location that has been recognized for several decades as the site of a structural discontinuity of the Aleutian arc. A channel known as the Amchitka pass separates the Andreanof Islands to the east, trending N78°E, from the Rat Islands group to the west, trending N110°E (Fig. 1). As a result, the subduction becomes more oblique to the west and the maximum depth of seismicity, reaching 250 km north of the Delarof Islands, tapers off to 180 km north of Amchitka and 135 km (with only three events below 100 km) west of Kiska (Engdahl *et al.* 1998). This geometry suggests that there exists at the very least a contortion, possibly a break, in the slab between longitudes 178°E and 179°W. Furthermore, longitude 180° effectively separates the inferred rupture zones of the megathrust events of 1965 and 1957 (Stauder 1968a; Johnson *et al.* 1994), and we know of no large earthquake whose rupture transgresses the Amchitka pass. This suggests that this locale may be acting as a 'barrier' (Aki *et al.* 1977) along the subduction zone, itself possibly controlled by a lateral heterogeneity in the subduction process.

In this respect, we note that the epicentral area coincides with the intersection of the Aleutian chain with the Bowers ridge, a horn-shaped, arcuate feature extending 500 km into the Bering sea (Fig. 1). It is generally thought to be the remnants of a volcanic arc formed at a fossil subduction system (Kienle 1971; Karig 1972; Scholl *et al.* 1975), but conflicting models have been proposed regarding the location and timing of its generation (Ben-Avraham & Cooper 1981; Cooper *et al.* 1992). The shallow structure of the Bowers ridge has been determined from a variety of studies (Kienle 1971; Ludwig *et al.* 1971; Cooper *et al.* 1981). Its crust reaches a thickness of 29 km and one can only speculate as to the depth of any mantle root it may have kept to this day, notably in view of intriguing results obtained under other fossil volcanic structures (VanDecar *et al.* 1995; Richardson *et al.* 2000). The existence of the Bowers

Table 2. Resolving the focal mechanism indeterminacy of the Aleutian event using body wave radiation coefficients.

Parameter	Mechanism I	Mechanism III	2003 Event November 17	1965 Main shock February 4	1965 Aftershock March 30
Strike ϕ_f, dip δ, slip λ (°)	196, 80, 304	16, 80, 124	281, 18, 122	290, 18, 139	104, 47, 242
Conjugate solution	300, 35, 198	120, 35, 18	68, 75, 80	60, 78, 76	322, 50, 297
R^P at TOK	0.74	0.51	0.48	0.58	−0.58
Observed	POSITIVE	POSITIVE	POSITIVE	POSITIVE	Positive
R^P at OSK	0.71	0.55	0.52	0.61	−0.64
Observed	POSITIVE	POSITIVE	POSITIVE	POSITIVE	Positive
R^{SV} at TOK	−0.59	0.37	0.19	0.09	−0.62
R^{SH} at TOK	−0.24	−0.46	−0.69	−0.69	0.51
R^E at TOK	0.29	−0.58	−0.60	−0.52	0.80
Observed	POSITIVE	Positive	Positive	Positive	POSITIVE
R^E at OSK	0.32	−0.55	−0.57	−0.49	0.75
Observed	POSITIVE	Positive	Positive	Positive	POSITIVE
R^N at TOK	0.57	0.10	0.40	0.46	0.02
Observed	POSITIVE	POSITIVE	POSITIVE	POSITIVE	Positive

Notes: mechanisms II and IV are not listed as they are the exact opposites of I and III, respectively, and thus all radiation coefficients are simply the negatives of their counterparts for I and III. The conventions for orienting R^{SV} and R^{SH} are those of Kanamori & Stewart (1976). Observed polarities are capitalized when correctly predicted by the model.

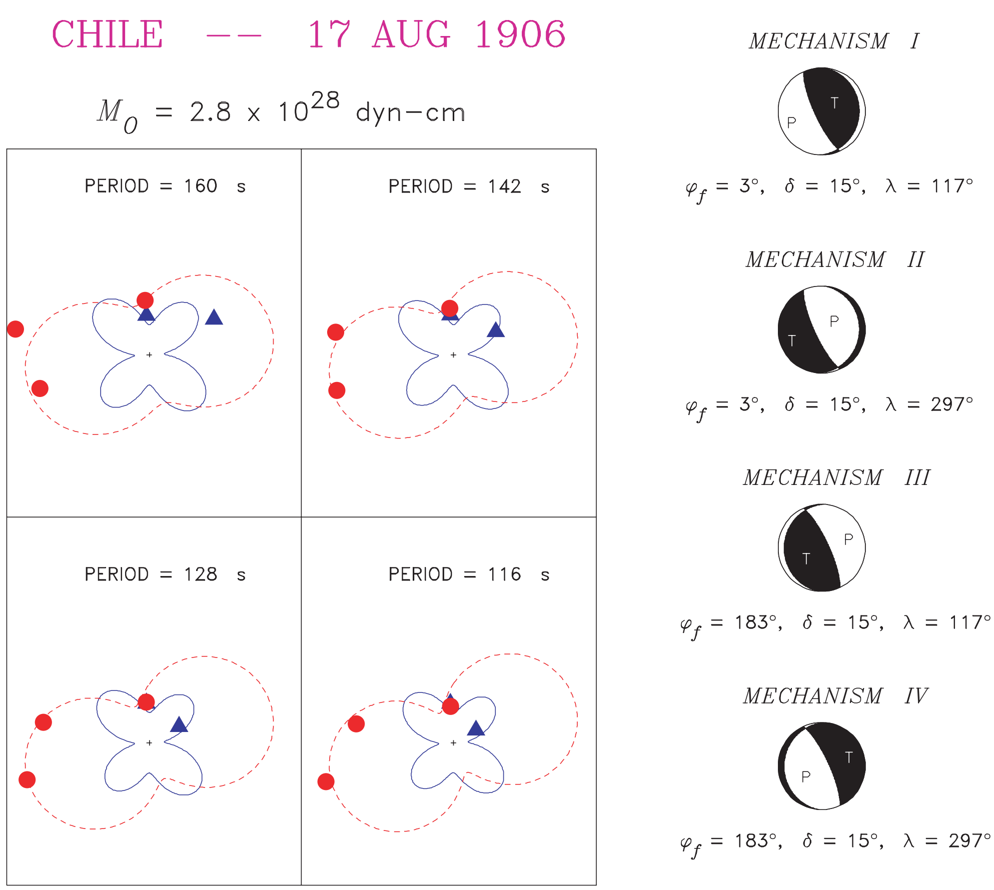

Figure 9. Result of the Preliminary Determination of Focal Mechanisms (PDFM) inversion for the Chilean event. The same conventions as on Fig. 6.

ridge could provide a framework for the development of a lateral heterogeneity in the subduction process, which in turn could lead to tearing of the slab, either by actual collision with an existing root, or under loading by the ridge structure. Such a context could possibly explain the location of the large intraslab earthquake of 1906.

Finally, the slip motion inverted in the present study is in general agreement with the deformation described by Geist *et al.* (1988);

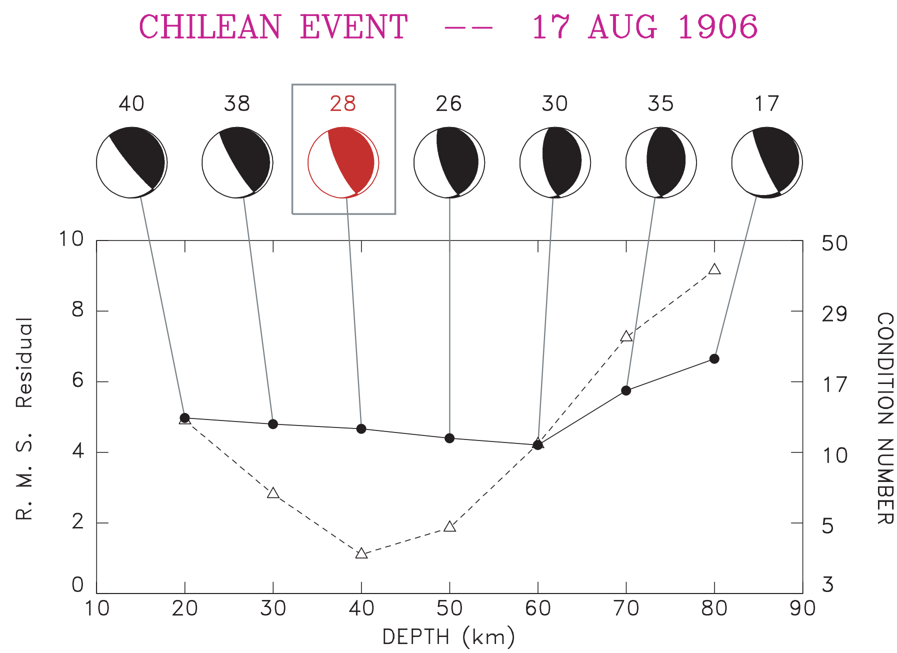

Figure 10. The same as Fig. 7 for the Chilean event.

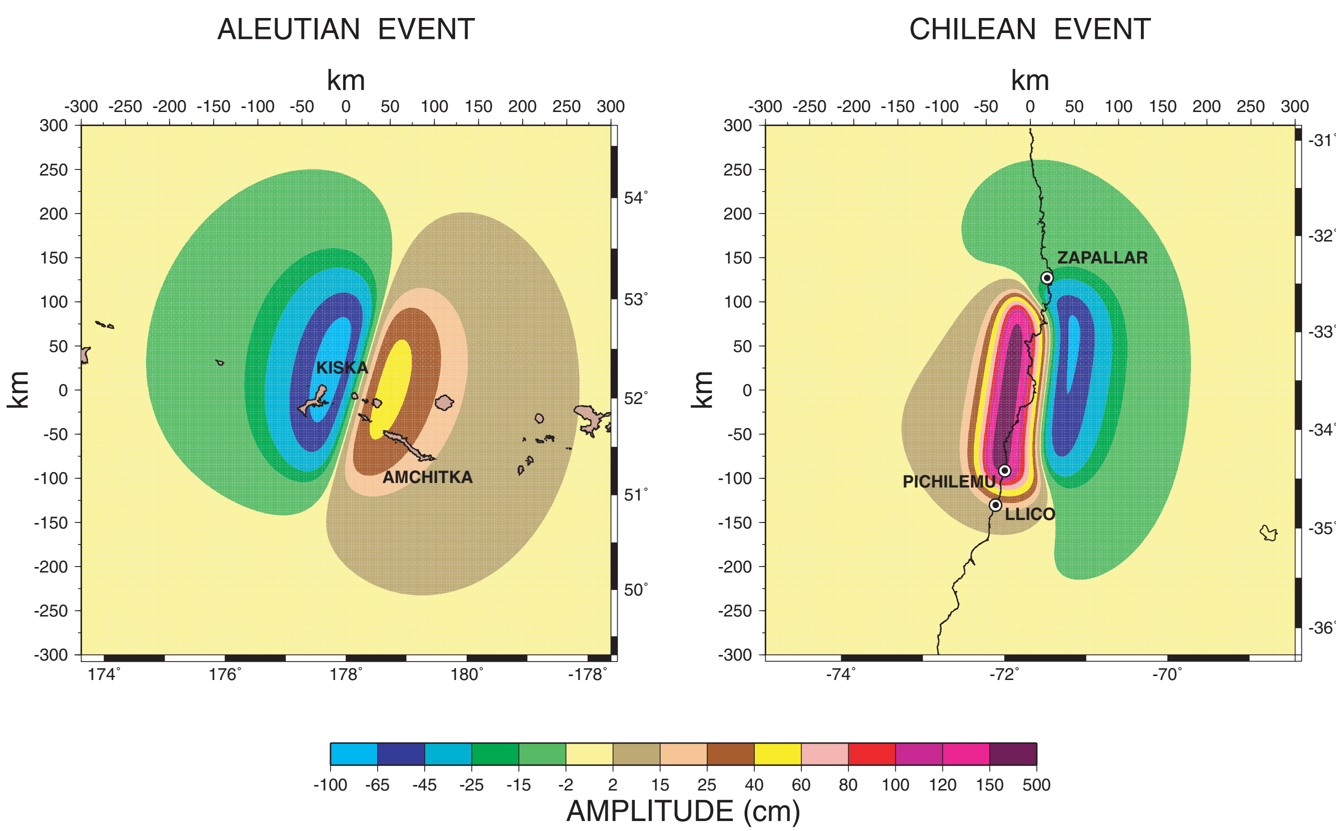

Figure 11. Models of static vertical ground displacement computed for the Aleutian (a) and Chilean (b) earthquakes. The individual Aleutian islands are superimposed on the map; in the case of Chile, only the coastline is shown, with the locations of uplift mentioned by Steffen (1907b) shown as bull's-eye symbols.

as part of a pattern of block rotation of various provinces of the Aleutian Islands, these authors proposed a left-lateral strike-slip motion oriented ∼30° NE at the eastern edge of the Rat Island block. An earthquake on 1966 July 4 in the Amchitka pass has precisely this mechanism (Stauder 1968a). It may be speculative to extrapolate this general motion to the inferred hypocentre of the 1906 event, but we cannot fail to notice that it is in agreement with the large strike-slip component of mechanism I.

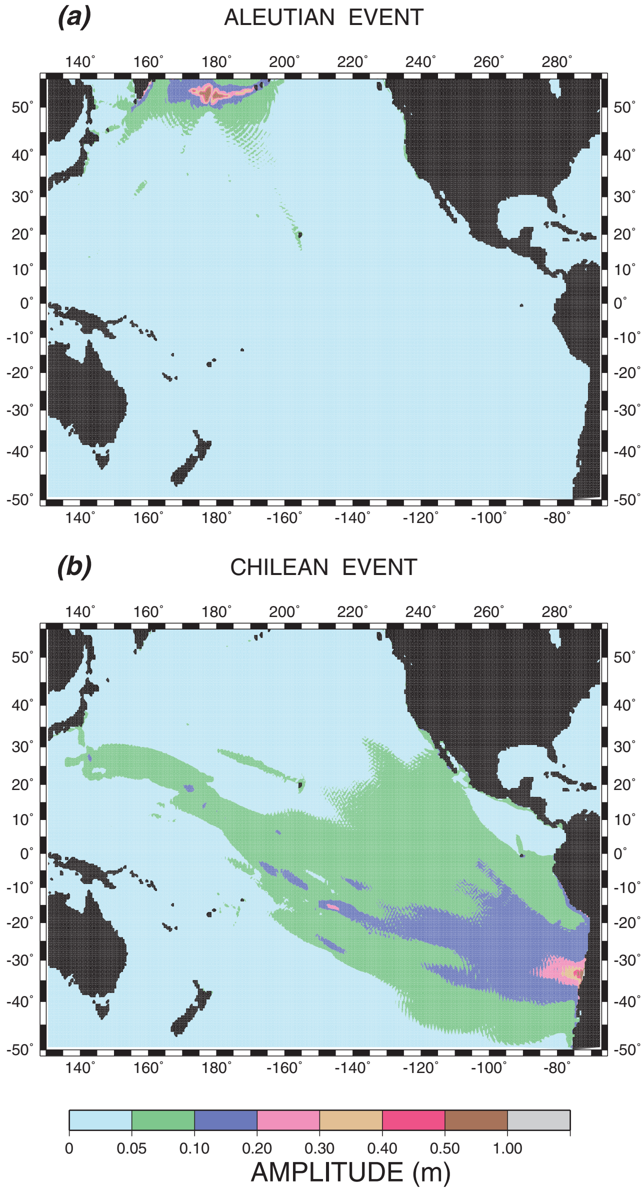

Figure 12. Far-field tsunami simulations for the Aleutian (a) and Chilean (b) events. Contoured is the maximum amplitude of the disturbance of the ocean surface for a period of 24 hr following the earthquake. Note the significant difference between the two sources in the far field. These simulations support the observation that the tsunami was generated by the Chilean earthquake, despite a smaller seismic moment than the Aleutian one.

4.3 Simulating the tsunami

In this section, we use our inverted focal geometries to consider plausible models of surface deformation and in turn simulate the transpacific tsunamis expected from our solutions. We justify that the Aleutian earthquake, despite featuring the larger of the two moments, generates a negligible transpacific tsunami, on account of its depth and location in the backarc.

For the Aleutian event, we take the steep plane in mechanism I (Fig. 6) as the fault plane and model a source rupturing from 40 to 102 km depth, with a fault length of 200 km, a slip of 4 m and a rigidity $\mu = 7 \times 10^{11}$ dyn cm^{-2}, adequate for an upper-mantle event. We use the algorithm of Mansinha & Smylie (1971) to infer the resulting vertical surface deformation field in the epicentral area, whose extrema are -75 and $+46$ cm, in the vicinity of Kiska and western Amchitka, respectively (Fig. 11a).

In turn, the resulting displacement field is used as an initial condition for a hydrodynamic computation using the Method Of Splitting Tsunami (MOST) algorithm, which solves the non-linear shallow-water wave equations on a variable staggered grid with the method of fractional steps (Titov & González 1997; Titov & Synolakis 1998); a full description is given in Synolakis (2002). Our simulations are carried out in a region extending from 50°S to 56°N and from 130°E to 60°W, using Smith & Sandwell's (1997) 2-min bathymetric grid. The tsunami is propagated for 24 hr in the Pacific ocean. Fig. 12(a) shows the field of maximum amplitude of the tsunami wave on the high seas. It is clear that it falls below 5 cm after approximately 1500 km or 2 hr.

For the Chilean event, we model a source rupturing from 23 to 45 km depth, with a fault length of 200 km and a slip of 5.3 m, with $\mu = 4.4 \times 10^{11}$ dyn cm^{-2}, adequate for a source in the crust. We use a focal geometry ($\phi_f = 8°$, $\delta = 17°$, $\lambda = 117°$) slightly rotated from mechanism I, but remaining in the range of scatter as a result of fluctuations in instrument response. This predicts extremal vertical motions of $+1.83$ m and -68 cm (Fig. 11b). We position the source to best reproduce the strong uplift at Pichilemu (at least 2.5 m) and the minimal one at Llico (40 cm) reported by Steffen (1907b). While we obtain a tentative fit of the order of magnitude of these displacements (Fig. 11b), we fail to reproduce the uplift reported farther north at Zapallar (80 cm). This misfit is most probably the result of source complexity and consequent slip heterogeneity on the fault plane. Using this displacement field as an initial condition, the tsunami simulation is carried out for 24 hr in the Pacific ocean. Fig. 12(b) shows the resulting maximum amplitude on the high seas. In the absence of detailed simulation of the response of specific bays and harbours, it is impossible to model the signals recorded at individual tide gauge stations, but the comparison of the two frames of Fig. 12 clearly shows that the Chilean source is a far more efficient far-field tsunami generator than the Aleutian one, despite an overall lower seismic moment, as expected from the deeper Aleutian focus and the location of the latter under the arc, its fault zone extending under the Bering sea and funneling little tsunami energy into the Pacific basin.

5 CONCLUSION

The exceptional collection of seismograms compiled by Rudolph & Tams (1907) allows the resolution of the focal mechanisms of the two great earthquakes of 1906 August 17. The available data sets of compiled arrival times are of somewhat lesser value, because of their inherent scatter and of inconsistencies between various versions. We find that the Chilean event is a regular interplate thrust earthquake, but its moment, the lesser of the two, suggests a significantly shorter rupture length (~200 km) than previously advocated; it was nevertheless the source of the transpacific tsunami. As for the Aleutian event, we confirm that it can be neither an interplate, nor a tensional outer-rise earthquake, based on mantle wave radiation patterns and body wave polarities in Japan. Following the 1994 Shikotan earthquake, Tanioka *et al.* (1995) had raised the possibility that 'many large events like (the Shikotan earthquake) occurred in the past but (had) been mistaken for underthrusting earthquakes'. We believe that the 1906 Aleutian earthquake represents exactly this scenario.

Finally, no study of the 1906 events can evade the mention of a possible triggering of the Chilean earthquake by the Aleutian one;

this question is raised inexorably by their exceptional simultaneity, in the sense that the second earthquake took place during the passage in its epicentral area of body wavefronts from the first one. As first proposed by Chinnery (1963) and reviewed most recently by Stein (1999), it has become increasingly clear that mechanisms of stress transfer do exist and take place for the triggering of one earthquake by a previous shock, in the local to regional field. However, improvements to this class of models, including those involving viscoelastic and poroelastic effects, have been successfully used only in the regional field (Hill *et al.* 1993; Pollitz & Sacks 1997), or at most along an extended but continuous plate boundary (Stein *et al.* 1997; Pollitz *et al.* 1998). Alternating cycles of seismicity on a global scale (which could be regarded as a form of teleseismic triggering) have been recognized only on a timescale of years to decades and, at any rate, lack a clear understanding of their mechanism (Romanowicz 1993). In this framework and in order to be convincing, any investigation of the admittedly fascinating suggestion that the 1906 events may somehow be related to each other would have to reconcile the following facts.

(i) Why only one occurrence? There have been more than 130 earthquakes with $h \leq 100$ km and at least one reported $M \geq 8$ in the past 110 yr, yet only the 1906 twins are separated by less time than the typical duration of a classical seismogram (~1 hr, corresponding to the passage of the major body waves and minor-arc surface waves). The immediate runner-up couples (1901 August 9 in Vanuatu and the Kuriles, and 1902 September 22–23 in the Marianas and Mexico) are separated by much longer intervals (5.5 and 43 hr, respectively) and at any rate the magnitudes of their first events, reported as 8.4 (Vanuatu) and 8.1 (Marianas), are eminently suspect, given the low magnitudes of present-day seismicity in loosely coupled subduction zones.

(ii) Why not the bigger earthquakes? At only 3.9×10^{28} dyn cm, the 1906 Aleutian earthquake is far from being gigantic and much larger events (1960 Chile, 1964 Alaska) did indeed generate significantly larger teleseismic displacements, strains and stresses in principle capable of affecting potentially seismogenic areas in the far field. Yet the 1960 Chilean earthquake was not followed by a distant $M \geq 8$ event for more than 3 yr (1963 Kuriles) and the 1964 Alaska earthquake for 313 days (1965 Rat Island).

(iii) Why would seismic waves be a good trigger? The Aleutian body waves transiting the epicentral area of the Chilean earthquake at the time of its rupture are not expected to produce strong motion (because of attenuation along the seismic path), but could still conceivably affect local stresses. In this respect, their effect would be most similar to that of solid Earth tides. Despite decades of numerous investigations, there is still no consensus on the topic of tidal triggering of earthquakes, with the most recent results suggesting at best a very weak correlation (Vidale *et al.* 1998a,b); because of undersampling, no conclusion can be drawn for large ($M \geq 8$) earthquakes. If there is no definitive evidence that large earthquakes can be triggered by tides, then why would relatively moderate waves from distant events do the job?

Because we can provide no acceptably deterministic answer to any of these questions, we prefer to consider the simultaneity of the two shocks as a random occurrence.

ACKNOWLEDGMENTS

More than a decade ago, Michel Cara originally revealed to me the existence of the Rudolph & Tams (1907) report and collection. I thank Ota Kulhánek for hosting me at the Seismological Observatory of the University of Uppsala, where the UPP records were directly digitized from the originals, many years ago. David Scholl provided a tutorial by e-mail on the intriguing presence and history of the Bowers ridge. The staff at the interlibrary loan desk of Northwestern University are thanked for providing a regular flow of the most arcane historical references. I am grateful to Abraham Lerman for help with translation and to Ms Anne Harpham at the Library of the Honolulu Advertiser for access to their excellent archives. The MOST code was kindly made available by Costas Synolakis. Many figures were drafted using the GMT software (Wessel *et al.* 1991). This research was partly supported by the National Science Foundation, under grant CMS-03-01054. Finally, the paper was improved by the comments of two anonymous reviewers.

REFERENCES

Abe, K., 1981. Magnitudes of large shallow earthquakes from 1904 to 1980, *Phys. Earth planet. Int.,* **27,** 72–92.

Abe, K. & Noguchi, S., 1983a. Determinations of magnitude for large shallow earthquakes, 1897–1917, *Phys. Earth planet. Int.,* **32,** 45–59.

Abe, K. & Noguchi, S., 1983b. Revision of magnitudes of large shallow earthquakes, 1897–1912, *Phys. Earth planet. Int.,* **33,** 1–11.

Aki, K., Bouchon, M., Chouet, B. & Das, S., 1977. Quantitative prediction of strong motion for a potential earthquake fault, *Ann. Geofis.,* **30,** 341–368.

Beck, S.L. & Christensen, D.H., 1991. Rupture process of the February 4, 1965, Rat Islands earthquake, *J. geophys. Res.,* **96,** 2205–2221.

Beck, S., Barrientos, S., Kausel, E. & Reyes, M., 1998. Source characteristics of historic earthquakes along the central Chile subduction zone, *J. S. Am. Earth Sci.,* **11,** 115–129.

Ben-Avraham, Z. & Cooper, A.K., 1981. Early evolution of the Bering Sea by collision of oceanic rises and North Pacific subduction zones, *Geol. Soc. Am. Bull.,* **92**(7), Part I, 485–495.

Boyd, T.M. & Lerner-Lam, A.L., 1988. Spatial distribution of turn-of-the-century seismicity along the Alaska-Aleutian arc, *Bull. seism. Soc. Am.,* **78,** 636–650.

Chinnery, M.A., 1963. The stress changes that accompany strike-slip faulting, *Bull. seism. Soc. Am.,* **53,** 921–932.

Comte, D., Eisenberg, A., Lorca, E., Pardo, M., Ponce, L., Saragoni, R., Singh, S.K. & Suárez, G., 1986. The 1985 Central Chile earthquake: a repeat of previous great earthquakes in the region?, *Science,* **233,** 449–453.

Cooper, A.K., Marlow, M.S. & Ben-Avraham, Z., 1981. Multichannel seismic evidence bearing on the origin of Bowers Ridge, Bering Sea, *Geol. Soc. Am. Bull.,* **92**(7), Part I, 474–484.

Cooper, A.K., Marlow, M.S., Scholl, D.W. & Stevenson, A.J., 1992. Evidence for Cenozoic crustal extension in the Bering Sea region, *Tectonics,* **11,** 719–731.

Engdahl, E.R., van der Hilst, R.D. & Buland, R.P., 1998. Global teleseismic earthquake relocation with improved travel times and procedures for depth determination, *Bull. seism. Soc. Am.,* **88,** 722–743.

Geist, E.L., Childs, J.R. & Scholl, D.W., 1988. The origin of summit basins of the Aleutian Ridge: Implications for block rotation of an arc massif, *Tectonics,* **7,** 327–341.

Geller, R.J., 1976. Scaling relations for earthquake source parameters and magnitudes, *Bull. seism. Soc. Am.,* **66,** 1501–1523.

Goodstein, J., Kanamori, H. & Lee, W.H.K., 1980. *Seismology records,* microfiche edn from the Caltech Archives, Calif. Inst. Tech., Pasadena.

Gutenberg, B. & Richter, C.F., 1954. *Seismicity of the Earth,* Princeton Univ. Press, Princeton, 310 pp.

Hill, D.P. *et al.*, 1993. Seismicity remotely triggered by the magnitude 7.3 Landers, California, earthquake, *Science,* **260,** 1617–1623.

Honda, K., Terada, T., Yoshida, Y. & Ishitani, D., 1908. Secondary undulations of oceanic tides, *J. Coll. Sci. Tokyo Univ.,* **24,** 1–113.

Johnson, J.M., Tanioka, Y., Ruff, L.J., Satake, K., Kanamori, H. & Sykes, L.R., 1994. The 1957 great Aleutian earthquake, *Pure appl. Geophys.,* **142,** 3–28.

Kagan, Y.Y., 1991. 3-D rotation of double-couple earthquake sources, *Geophys. J. Int.,* **106,** 709–716.

Kanamori, H., 1977. The energy release in great earthquakes, *J. geophys. Res.,* **82,** 2981–2987.

Kanamori, H. & Stewart, G.S., 1976. Mode of strain release along the Gibbs Fracture Zone, Mid-Atlantic Ridge, *Phys. Earth planet. Int.,* **11,** 312–332.

Karig, D., 1972. Remnant arcs, *Geol. Soc. Am. Bull.,* **83,** 1057–1068.

Kelleher, J.A., 1972. Rupture zones of large South American earthquakes and some predictions, *J. geophys. Res.,* **77,** 2087–2103.

Kienle, J., 1971. Gravity and magnetic measurements over Bowers Ridge and Shirshov Ridge, Bering Sea, *J. geophys. Res.,* **76,** 7138–7153.

Kikuchi, M. & Kanamori, H., 1995. The Shikotan earthquake of October 4, 1994: Lithospheric earthquake, *Geophys. Res. Lett.,* **22,** 1025–1028.

Lomnitz, C., 1970. Major earthquakes and tsunamis in Chile during the period 1535 to 1955, *Geol. Rundsch.,* **59,** 938–960.

Ludwig, W.J. *et al.*, 1971. Structure of Bowers Ridge, Bering Sea, *J. geophys. Res.,* **76,** 6350–6366.

Mansinha, L. & Smylie, D.E., 1971. The displacement fields of inclined faults, *Bull. seism. Soc. Am.,* **61,** 1433–1440.

Minster, J.-B., Jordan, T.H., Molnar, P. & Haines, E., 1974. Numerical modelling of instantaneous plate tectonics, *Geophys. J. R. astr. Soc.,* **36,** 541–576.

Nishenko, S.P., 1985. Seismic potential for large and great interplate earthquakes along the Chilean and southern Peruvian margins of South America; a quantitative reappraisal, *J. geophys. Res.,* **90,** 3589–3615.

Okal, E.A., 1992a. Use of the mantle magnitude M_m for the reassessment of the seismic moment of historical earthquakes. I: Shallow events, *Pure appl. Geophys.,* **139,** 17–57.

Okal, E.A., 1992b. A student's guide to teleseismic body-wave amplitudes, *Seism. Res. Lett.,* **63,** 169–180.

Okal, E.A. & Reymond, D., 2003. The mechanism of the great Banda Sea earthquake of 01 February 1938: Applying the method of Preliminary Determination of Focal Mechanism to a historical event, *Earth planet. Sci. Lett.,* **216,** 1–15.

Okal, E.A. & Synolakis, C.E., 2004. Source discriminants for near-field tsunamis, *Geophys. J. Int.,* **158,** 899–912.

Okal, E.A. & Talandier, J., 1989. M_m: A variable period mantle magnitude, *J. geophys. Res.,* **94,** 4169–4193.

Okal, E.A. & Talandier, J., 1990. M_m: Extension to Love waves of the concept of a variable-period mantle magnitude, *Pure appl. Geophys.,* **134,** 355–384.

Omori, F., 1907. Notes on the Valparaiso and Aleutian earthquakes of August 17, 1906, *Bulletin of the Imperial Earthquake Investigating Committee,* **1,** 75–113.

Pacific Commercial Advertiser, 1906. Twelve-foot tidal wave on Maui coast, *Pacific Commercial Advertiser,* 1906 August 17 and 18.

Plafker, G.L., 1985. Geologic reconnaissance of the March 3, 1985, Chile earthquake, *US Geol. Surv. Open File Report,* **85–0542,** 13–20.

Pollitz, F.F. & Sacks, I.S., 1997. The 1995 Kobe, Japan earthquake: A long-delayed aftershock of the offshore 1944 Tonankai and 1946 Nankaido earthquakes, *Bull. seism. Soc. Am.,* **87,** 1–10.

Pollitz, F.F., Bürgmann, R. & Romanowicz, B., 1998. Viscosity of oceanic asthenosphere inferred from remote triggering of earthquakes, *Science,* **280,** 1245–1249.

Reymond, D. & Okal, E.A., 2000. Preliminary determination of focal mechanisms from the inversion of spectral amplitudes of mantle waves, *Phys. Earth planet. Int.,* **121,** 249–271.

Richardson, W.P., Okal, E.A. & van der Lee, S., 2000. Rayleigh-wave tomography of the Ontong-Java Plateau, *Phys. Earth planet. Int.,* **118,** 29–51.

Romanowicz, B.A., 1993. Spatiotemporal patterns in the energy release of great earthquakes, *Science,* **260,** 1923–1926.

Romanowicz, B.A. & Suárez, G., 1983. On an improved method to obtain the moment tensor and depth of earthquakes from the amplitude spectrum of Rayleigh waves, *Bull. seism. Soc. Am.,* **73,** 1513–1526.

Rudolph, E. & Tams, E., 1907. *Seismogramme des nordpazifischen und südamerikanischen Erdbebens am 16. August 1906,* DuMont Schauberg, Strasbourg, 98 pp.

Scholl, D.W., Buffington, E.C. & Marlow, M.S., 1975. Plate tectonics and the structural evolution of the Aleutian-Bering Sea region, *Geol. Soc. Am. Mem.,* **151,** 1–31.

Smith, W.H.F. & Sandwell, D.T., 1997. Global sea floor topography from satellite altimetry and ship depth soundings, *Science,* **277,** 1956–1962.

Solov'ev, S.L. & Go, Ch.N., 1984. Catalogue of tsunamis on the Eastern shore of the Pacific Ocean, *Can. Transl. Fish. Aquat. Sci.,* **5078,** 285 pp., Sidney, BC.

Stauder, W.J., 1968a. Mechanism of the Rat Island earthquake sequence of February 4, 1965, with relation to island arcs and sea-floor spreading, *J. geophys. Res.,* **73,** 3847–3858.

Stauder, W.J., 1968b. Tensional character of earthquake foci beneath the Aleutian trench with relation to sea floor spreading, *J. geophys. Res.,* **73,** 7693–7701.

Steffen, H., 1907a. Einige Ergebnisse der Untersuchungen über das mittelchilenische Erdbeben von 16. August 1906, *Pettermanns Mitteil.,* **53,** 132–138.

Steffen, H., 1907b. *Contribuciones para un estudio cientifico del terremoto del 16 de agosto de 1906,* Cervantes, Santiago, 83 pp.

Stein, R.S., Barka, A.A. & Dieterich, J.H., 1997. Progressive failure on the North Anatolian fault since 1939 by earthquake stress triggering, *Geophys. J. Int.,* **128,** 594–604.

Stein, R.S., 1999. The role of stress transfer in earthquake occurrence, *Nature,* **402,** 605–609.

Synolakis, C.E., 2002. Tsunami and seiche, in *Earthquake engineering handbook,* pp. 9-1–9-90, eds Chen, W.-F. & Scawthorn, C., CRC Press, Boca Raton.

Tanioka, Y., Ruff, L.J. & Satake, K., 1995. The great Kurile earthquake of October 4, 1994 tore the slab, *Geophys. Res. Lett.,* **22,** 1661–1664.

Tarantola, A., 1987. *Inverse problem theory: methods for data fitting and model parameter estimation,* Elsevier, Amsterdam, 613 pp.

Titov, V.V. & González, F.I., 1997. Implementation and testing of Method Of Splitting Tsunami (MOST) model, *NOAA Technical Memorandum ERL-PMEL,* **112,** 111 pp.

Titov, V.V. & Synolakis, C.E., 1998. Numerical modeling of tidal wave runup, *Journal of Waterway, Port and Coastal Engineering,* **B124,** 157–171.

VanDecar, J.C., James, D.E. & Assumpção, M., 1995. Seismic evidence for a fossil mantle plume beneath South America and implications for plate driving forces, *Nature,* **378,** 25–31.

Vidale, J.E., Agnew, D.C., Johnston, M.S.J. & Oppenheimer, D.H., 1998a. Absence of earthquake correlation with Earth tides: An indication of high preseismic fault stress rate, *J. geophys. Res.,* **103,** 24 567–24 572.

Vidale, J.E., Agnew, D., Rodriguez, C. Oppenheimer, D. & Houston, H., 1998b. A weak correlation between earthquakes and extensional normal stress and stress rate from lunar tides, *EOS, Trans. Am. geophys. Un.,* **79**(45), F640 (abstract).

Wessel, P. & Smith, W.H.F., 1991. Free software helps map and display data, *EOS, Trans. Am. geophys. Un.,* **72,** 441 and 445–446.

Wu, F. & Kanamori, H., 1973. Source mechanism of February 4, 1965 Rat Island earthquake, *J. geophys. Res.,* **78,** 6082–6092.

Wysession, M.E., Okal, E.A. & Miller, K.L., 1991. Intraplate seismicity of the Pacific Basin, 1913–1988, *Pure appl. Geophys.,* **135,** 261–359.

Zöppritz, K., 1906. *Wöchentliche Erdbebenberichte des geophysikalischen Instituts der Universität Göttingen,* no. 47, University of Göttingen, Göttingen.

APPENDIX A: THE CASE OF THE REPORT OF 3.5 m AT MAUI

The run-up of 3.5 m at Maui (Solov'ev & Go 1984) constitutes the largest value reported Pacific-wide for the tsunami associated with the twin events. Because it dwarfs the amplitudes on the Chilean coast, it motivated Lomnitz (1970) to propose that the tsunami was generated by the Aleutian event, for which no near-field run-up data is available. Abe's (1981) use of the figure of 3.5 m also resulted in a significant over estimate of the moment of the Chilean event. Finally, this height is in disagreement with other records in the Hawaiian

Islands. In this context, we decided to investigate in detail the sources of the report of Solov'ev & Go (1984).

The inundation of the coast of Maui is reported in the daily newspaper Pacific Commercial Advertiser (1906; now the Honolulu Advertiser) as the front page lead story of their issue for 1906 August 17, Friday, under the title 'Twelve-foot tidal wave on Maui coast'. The crucial information is the dateline of the article, 'KAHULUI, August 16.—2:10 p.m.', which has to be posterior to the inundation itself. The earliest arrival time at Maui for an Aleutian-generated tsunami would be 05:10 GMT, or 18:43 (6:43 pm on August 16), solar time in Maui. For a Chilean-generated tsunami, these times would be 13:37 GMT, or 03:10 solar time on August 17 in Maui. Although there remains the usual uncertainty as to the exact time being used in the Hawaiian Islands in 1906, an association of the reported phenomenon with the Aleutian earthquake would require that the time in use in Maui be at least 4.5 hr behind the Sun, which we dismiss. For the Chilean event to be the origin of the Maui wave, the clocks would have to be more than 13 hr behind the Sun.

We conclude that the wave at Maui is non-causal with respect to both events and that its origin must thus be sought in an independent phenomenon, which could have been a local underwater landslide. Additional evidence to support this interpretation includes the following.

(i) The report of the Chilean-generated tsunami at Hilo (with run-up of 1.5 m), from the next day's (1906 August 18, Saturday) edition of the newspaper, datelined 'HILO, August 17' (no time given): 'There was a five-foot tidal wave at Hilo this morning', which is in agreement with travel times from Chile, but suffers a discrepancy of at least 10 hr with the report at Maui; they cannot be the result of the same source.

(ii) The extreme spatial concentration of the damage by the wave on Maui. As reported in the Pacific Commercial Advertiser (1906), the wharf at Maalea bay was 'destroyed', that at McGregor Landing (about 7 km away) was 'damaged' and there was 'no particular damage' at Lahaina, 13 km farther away along the coast. While the non-linear response of the concave shoreline along Maalea bay may have enhanced run-up, such large lateral gradients in run-up distributions are characteristic of near-field tsunamis generated by landslides (Okal & Synolakis 2004).